Method transfer from high-pressure liquid chromatography to ultra-high-pressure liquid chromatography. II. Temperature and pressure effects

Dennis Åsberg[1], Jörgen Samuelsson[1*], Marek Leśko[2], Alberto Cavazzini[3], Krzysztof Kaczmarski[2*] and Torgny Fornstedt[1]

[1]Department of Engineering and Chemical Sciences, INTERACT, Karlstad University, SE-651 88 Karlstad, Sweden

[2]Department of Chemical and Process Engineering, Rzeszów University of Technology, PL-35 959 Rzeszów, Poland

[3]Department of Chemical and Pharmaceutical Sciences, University of Ferrara, IT-44 121 Ferrara, Italy

*Corresponding authors' information:

J. Samuelsson: Phone: +46 54 700 1620; fax: + 46 73 271 2890; email: Jorgen.Samuelsson@kau.se.

K. Kaczmarski: Phone: +48 17 865 1295; fax: +48 17 854 3655; email: kkaczmarski@prz.edu.pl.

Abstract

The importance of the generated temperature and pressure gradients in ultra-high-pressure liquid chromatography (UHPLC) are investigated and compared to high-pressure liquid chromatography (HPLC). The drug Omeprazole, together with three other model compounds (with different chemical characteristics, namely uncharged, positively and negatively

charged) were used. Calculations of the complete temperature profile in the column at UHPLC conditions showed, in our experiments, a temperature difference between the inlet and outlet of 16°C and a difference of 2°C between the column center and the wall. Through van't Hoff plots, this information was used to single out the decrease in retention factor (*k*) solely due to the temperature gradient. The uncharged solute was least affected by temperature with a decrease in *k* of about 5% while for charged solutes the effect was more pronounced, with *k* decreases up to 14%. A pressure increase of 500 bar gave roughly 5% increase in *k* for the uncharged solute, while omeprazole and the other two charged solutes gave about 25, 20 and 15% increases in *k*, respectively. The stochastic model of chromatography was applied to estimate the dependence of the average number of adsorption/desorption events (*n*) and the average time spent by a molecule in the stationary phase (τ_s) on temperature and pressure on peak shape for the tailing, basic solute. Increasing the temperature yielded an increase in *n* and decrease in τ_s which resulted in less skew at high temperatures. With increasing pressure, the stochastic modelling gave interesting results for the basic solute showing that the skew of the peak increased with pressure. The conclusion is that pressure effects are more pronounced for both retention and peak shape than the temperature effects for the polar or charged compounds in our study.

Keywords: Liquid chromatography; Method transfer; UHPLC; Pressure; Temperature; Stochastic theory.

1 Introduction

The interest from the industry to move analytical methods from high-pressure liquid chromatography (HPLC) to ultra-high-pressure liquid chromatography (UHPLC) has grown in the last five years [1]. UHPLC provides faster separations and lower solvent consumption

compared to HPLC, with preserved column efficiency [2,3]. This is achieved by decreasing the particle size of the stationary phase and increasing the linear velocity of the mobile phase. As a consequence, the pressure drop over the column is much larger in UHPLC compared to HPLC, which leads to significant pressure and temperature (due to viscous heating and solvent compression) gradients in the column. These gradients have been shown to affect chromatographic performance and predictability [4].

Temperature gradient depends strongly on the method employed to thermostat the column and has been calculated for different conditions in UHPLC [5–9]. Longitudinal temperature gradients prevail when the column compartment is close to adiabatic (e.g. in still-air conditions); they essentially affect only retention time, without compromising column efficiency. Radial temperature gradients, on the other hand, arise in well-thermostated conditions (e.g., with water thermostating), where the center of the column has a different temperature than the wall. Radial temperature gradients result in decreased column efficiency and should therefore be avoided.

The effect of typical pressures found in UHPLC (ca 1 000 bar) on retention has been investigated for a number of small compounds and large biomolecules [4,10,11]. For uncharged species, relatively small changes (of up to 12%) in retention factor were observed for a pressure increase of 500 bar. For polar or ionic solutes much larger increases, up to 50%, were reported.

Stochastic models of chromatography describe the chromatographic processes at a molecular level [12]. In these models, the chromatographic migration is represented as a random process in which each molecule, while migrating along the column, performs a random number of adsorption/desorption steps of random duration. Using the Characteristic Function formalism in the Fourier domain [13] the stochastic model have been used for studying heterogeneous adsorption, to including the effect of mobile phase

71 dispersion [14,15], reversed phase [16], chiral [17], size-exclusion [18], and ion-exchange
72 separations [19].

73 In this study, the pressure effect will be investigated from a stochastic point of view. It has
74 previously been shown that both efficiency and peak symmetry can decrease with increasing
75 pressure [20]. Applying the stochastic model at different pressures yield valuable insight in
76 how the peak shape and retention depend on pressure. This is especially true for
77 compounds exhibiting heterogeneous adsorption which, to our knowledge, have not been
78 studied at different pressures. For heterogeneous adsorption, the van't Hoff plot does not
79 yield any relevant physic-chemical information [21], so by also studying heterogeneous
80 adsorption at different temperatures using stochastic modelling the effect of pressure and
81 temperature gradients in UHPLC can be investigated for a heterogeneous adsorption
82 processes.

83 Additionally, by combining calculations of the temperature profile in the column with the
84 pressure and temperature dependence of retention factor individual contributions of
85 pressure and temperature effects can be determined in a more rigorous way than previously
86 described in the literature.

87 The aim of this study is to investigate the effect of pressure and temperature gradients by
88 calculating their gradients and determining the individual contributions to retention and
89 peak shape. Temperature and pressure effects are first investigated separately and then the
90 combined effect is studied using the same model compounds as in part I [22] (an uncharged,
91 a positively and a negatively charged and the drug omeprazole). To enable the study of
92 pressure and temperature effects for compounds with heterogeneous adsorption, stochastic
93 modelling will be used. Finally we will compare the retention time and efficiency between
94 HPLC and UHPLC for omeprazole and one degradation product.

2 Theory

The stochastic theory [15,23,24] describes the chromatographic process in terms of random variables, namely the time spent by a molecule on the stationary phase (sojourn time) and that elapsed between two successive adsorption/desorption events (flying time). The history of a molecule traveling through a column can be interpreted as the sum of a random number of adsorption/desorption steps performed by that molecule inside the column. Mathematically, for each molecule, this history will be the convolution integral of the density functions of the time spent on the site. By means of the properties of the Characteristic Function (i.e., the inverse Fourier transform of the probability density function) it is possible to substitute the convolution integral with the product of the elementary characteristic functions and to obtain both the fundamental peak shape parameters (mean, variance, skew, etc.) and the chromatogram itself. In the language of stochastic models, the chromatographic process is a Poisson process, the chromatographic peak being the probability density function of time spent in the column by molecules. Let us define the average number of adsorption/desorption events by n and the average sojourn and flying times by τ_s and τ_m, respectively. Under the previous hypotheses, it can be demonstrated that, for a homogeneous surface (that is one characterized by a single sorption site type), the average retention time is given by:

$$t_R = n\tau_m + n\tau_s \quad (1)$$

where $n\tau_m$ is the time spent, on average, by a molecule in the mobile phase (i.e., the column hold-up time) and $n\tau_s$ is the average time a molecule spends in the stationary phase.

For a heterogeneous surface, on the other hand, the corrected retention time will depend on both the characteristics of the different adsorption sites and their relative abundance on the phase. In the simple case of a surface paved with only two types of adsorption sites (2-site heterogeneous model [15]), the average retention time can be expressed as:

$$t_R = n\tau_m + n\left(p_1\tau_{s,1} + p_2\tau_{s,2}\right) \quad (2)$$

where p_i is the relative amount of the i:th site (i = 1, 2) and $n = n_1 + n_2$.

Through the characteristic function method, the calculation of statistical peak moments is straightforward [13,15]. Using this statistical moments it is possible to calculate the parameters traditionally used to describe peak asymmetry, such as peak skew or peak excess, and to obtain expressions for the height equivalent to a theoretical plate (H) or the number of theoretical plates (N). The skew (S) for the 1-site and the 2-site models are given by Eq. 3a and Eq. 3b, respectively [15]:

$$S = \frac{3}{2\sqrt{n}} \quad (3a)$$

$$S = \frac{3}{2\sqrt{n}} \frac{p_1\tau_{s,1}^3 + p_2\tau_{s,2}^3}{\left(p_1\tau_{s,1}^2 + p_2\tau_{s,2}^2\right)^{3/2}} \quad (3b)$$

Column efficiency is determined according to [15]:

$$\frac{1}{N} = \frac{1}{N_D} + \frac{2}{N_M}\left(\frac{k}{k+1}\right)^2 \quad (4)$$

where, k is the retention factor and N_D is the dispersion effect from the mobile phase estimated from an unretained marker fitted to the exponentially modified Gaussian distribution (EMG) and calculated from the distribution's mean and variance. N_M is defined for the 1-site model by:

$$N_M = n \quad (5a)$$

and for the 2-site model as:

$$N_M = n \frac{\left(p_1 + p_2 \left(\tau_{s,2} / \tau_{s,1}\right)\right)^2}{p_1 + p_2 \left(\tau_{s,2} / \tau_{s,1}\right)^2} \quad . \tag{5b}$$

To obtain pure data for calculations of adsorption/desorption kinetics, the extra column contribution to the elution zone must be removed. This was done by fitting the peak of the void volume marker to an exponentially modified Gaussian distribution and by deconvolution of the elution peak of the void volume contribution. In this work the stochastic model parameters were estimated using the super modified sequential simplex optimization by minimization of the least-squares errors [25]. In this context it is worth mentioning that the main objective for the stochastic models are to correlate the changes in peak asymmetry (tailing) with pressure and temperature - not to study band broadening itself. For the latter, if the band broadening is not tailed so much, general models/approaches that is sufficient [26].

3 Material and methods

3.1 Chemicals

The mobile phase was acetonitrile/aqueous-buffer (15 mM phosphate buffer, pH 8.00) mixtures. Gradient grade acetonitrile was purchased from VWR International (Radnor, PA, USA). The buffer was prepared from water with conductivity 5.5 µS/m delivered from a Milli-Q Plus 185 water purification system from Merck Millipore (Billerica, MA, USA) and from analytical grade sodium phosphate dibasic dihydrate and sodium phosphate monobasic dihydrate purchased from Sigma-Aldrich (St. Louis, MO, USA). The phosphate buffer was filtered through a 0.2 µm nylon filter membrane purchased from Whatman (Maidstone, UK) before it was mixed with acetonitrile. The amount of acetonitrile varied from 7 to 25% v/v, depending on the solute. Benzyltriethylammonium chloride, BTEAC, (99%), cycloheptanone, C7, (99%), sodium 2-naphtalenesulfonate, SNS, (≥95%), all from Sigma-Aldrich, and

161 omeprazole sodium monohydrate, OM, (>99%), kindly gifted by AstraZeneca (Mölndal,
162 Sweden), were used as solutes. BTEAC is positively charged, SNS is negatively charged and
163 C7 and OM are uncharged at pH 8. The column hold-up volume was determined with sodium
164 nitrate (≥99.0%) purchased from Sigma-Aldrich.

165 **3.2 Chromatographic equipment**

166 The HPLC system was an Agilent 1200 chromatograph (Agilent Technologies, Palo Alto, CA,
167 USA) equipped with a binary pump, an auto sampler, a diode-array UV-detector and a
168 thermostated still air column oven. The extra column volume from the auto sampler to the
169 detector was 0.037 mL and has been subtracted from the experimental data. The HPLC
170 column was a 100 × 4.6 mm XBridge BEH C_{18} column with an average particle diameter of 3.5
171 µm and column hold-up volume 0.97 mL. The physicochemical properties of the column are
172 reported in Table 1. As the column was thermostated in a still air compartment, it can be
173 assumed that it is under adiabatic conditions [9].

174 The UHPLC system was a Waters Acquity UPLC H-class (Waters Corporation, Milford, MA,
175 USA) equipped with quaternary pump system, an auto sampler, a diode-array UV-detector
176 and a thermostated column oven. Also in this case, one may assume the column to be under
177 adiabatic conditions. The extra column volume from the auto sampler to the detector was
178 0.027 mL and has been subtracted from the experimental data. The UHPLC column was a 50
179 × 2.1 mm Acquity UPLC BEH C_{18} with an average particle diameter of 1.7 µm. The physico-
180 chemical properties of the column are given in Table 1. The flow rates of the respective
181 systems used depended on the goals of the experiments and are mentioned in connection to
182 the actual experiment, below. As example, for fundamental studies in UHPLC we used a very
183 low flow rate to avoid pressure and temperature gradients whereas for optimized UHPLC
184 experiments we used a high flow rate.

185 ## 3.3 Temperature, mass flow and pressure measurements

186 The temperature of the column wall was measured by attaching three PT-100 (4-wire)
187 resistance temperature detectors from Pentronic AB (Gunnebo, Sweden) directly on the
188 column surface. For the UHPLC column, they were attached on the column wall at 10.7, 21.9
189 and 35.0 mm from the column inlet and for HPLC they were placed at 21 and 81 mm from
190 the inlet. A thermal adhesive from Arctic Silver Inc. (Visalia, CA, USA) was used to attach
191 them. The PT-100 elements had the accuracy ±0.2°C and were verified in house against a
192 reference thermometer.

193 The total mass flow was measured by connecting a mini CORI-FLOW Coriolis mass flow
194 meter after the detector which was purchased from Bronkhorst High-Tech B.V. (Ruurlo,
195 Netherlands) and had accuracy equal to ±0.2% of the mass flow.

196 The pressure at the column inlet and outlet was determined by repe ating the experiments
197 first with the capillary going to the column inlet reconnected directly to waste and then with
198 the column replaced by a zero-volume union. The temperature was measured at the flow
199 rates 0.25, 0.50, 1.00 and 1.20 mL/min for UHPLC and at 0.40 and 1.00 mL/min for HPLC. The
200 mobile phase was 25% acetonitrile as this composition corresponds to the largest viscosity
201 of the mobile phase [27].

202 ## 3.4 Calculating temperature profiles

203 The experimentally measured axial temperature difference between column inlet and outlet
204 was less than 0.5°C in HPLC at flow rate ≤ 1 mL/min and in UHPLC at flow rate ≤ 0.25
205 mL/min. This temperature difference is deemed negligible so these conditions were not
206 modelled.

207 The modelling of temperature profiles in chromatographic columns was done with the same
208 method as described in refs. [8,9]. This method combines models of heat and mass transfer

209 and mobile phase velocity distribution. In these calculations, the mass flow measured
210 externally was used in place of the set up volumetric flow rate. The external heat transfer
211 coefficient and the parameter in the Blake-Kozeny-Carman correlation were estimated by
212 minimizing the differences between calculated and experimental values of column outlet
213 pressure and temperature (measured at the third temperature sensor). The external heat
214 transfer coefficient was equal to 30 W/(m^2 K) and the Blake-Kozeny-Carman parameter was
215 146. At the different flow rates, calculations were validated by comparing the estimated
216 temperature at the column wall (at the positions of the temperature sensors) with the
217 experimental temperatures. The agreement between calculated and experimental data was
218 very satisfactory, with relative errors smaller than 0.5%.

219 **3.5 Chromatographic experiments**

220 Triplicate analytical injections of the four compounds were done at different temperatures
221 in HPLC and UHPLC and for different pressures for UHPLC. BTEAC (0.01 g/L) was studied at
222 7% acetonitrile in the eluent, SNS (0.001 g/L) at 15% and C7 (1 g/L) and OM (0.025 g/L) at
223 25%. The column hold-up volume was measured with $NaNO_3$ (0.005 g/L) before each
224 injection. In HPLC it was equal to 1.00, 0.96 and 0.93 mL and in UHPLC it was 0.11, 0.10, 0.10
225 mL for 7%, 15% and 25%, respectively. Injection volumes were 5 µL in HPLC and 2 µL in
226 UHPLC while all compounds were detected at 220 nm except C7, which was detected at 280
227 nm. The flow rates were 1.00 and 0.13 mL/min in HPLC and UHPLC, respectively, which
228 resulted in maximum pressure drops of 150 and 100 bar over the columns (negligible
229 pressure and temperature gradients).

230 When investigating the effect of temperature, the temperature was changed in 5°C
231 increments and analytical peaks were recorded at each temperature. The interval for HPLC
232 was 20-40°C and for UHPLC 30-50°C. The intervals were different due to different technical
233 limitations: the HPLC column thermostat was unable to have stable temperatures > 40°C

while the UHPLC thermostat could not operate in a reliable way at temperature < 25°C. The pressure was studied by placing a restriction capillary between the column outlet and the detector. The extra column contributions from the restriction capillaries were measured and accounted for in the calculations, by lifting out the column and injecting the sample at each restriction capillary set up. As restriction capillaries LC PEEKsil tubing with inner diameter 25 ± 1 µm from SGE Analytical Science (Milton Keynes, U.K.) was used with lengths 5, 10, 15 and 20 cm. This approach allows to minimizing pressure and temperature gradients over the column. The pressure used in the calculations is taken as the average pressure in the column when assuming a linear pressure drop over the column [28] and is denoted P_{avg} It is calculated as:

$$P_{avg} = \frac{P_{col.\,inlet} - P_{col.\,outlet}}{2} + \Delta P_{after\,col.} \quad (6)$$

where $P_{col.\,inlet}$ and $P_{col.\,outlet}$ is the pressure at the column inlet and outlet while $\Delta P_{after\,col.}$ is the total pressure drop from the column outlet to atmosphere including the restriction capillary. The pressures in Eq. 6 were determined separately for all experimental systems. Five different pressures were investigated for each solute; $P_{avg,\,25\%}$ = 53, 174, 302, 420, 550 bar, $P_{avg,\,15\%}$ = 53, 175, 314, 419, 552 bar and $P_{avg,\,7\%}$ = 51, 167, 301, 398, 524 bar, where the "%" denotes the fraction of acetonitrile in the mobile phase.

4 Results and discussion

To demonstrate that a direct method transfer from HPLC to UHPLC is not always straightforward, the four compounds employed in this work have been eluted on the two columns under isocratic conditions and typical flow rates of HPLC and UHPLC (1.0 and 1.2 ml/min, respectively). It is worth to mention that these flow rates were not obtained as the optimal flow rate in a van Deemter curve, as the study of column efficiency was not the

purpose of this work. Temperature in both cases was set to 40°C. Overlaid chromatograms are presented in Fig. 1 where, for the sake of comparison, retention is expressed as column volumes instead of retention time. It is evident from Fig. 1 that the retention in column volumes is longer for UHPLC (gray lines) compared to HPLC (black lines), especially for the late eluting peaks which also exhibit more tailing in UHPLC. This difference in retention might be caused by factors such as different pressures, temperature gradients and column chemistry. From calculating the efficiency with the moment method for HPLC and UHPLC in Fig. 1, it could be seen that, in this case, HPLC condition yielded the highest efficiency. The average efficiency of three injections were for HPLC 6230, 9430, 10730 and 9330 and for UHPLC 1610, 3560, 5050 and 4330 for BTEAC, SNS, C7 and OM, respectively. Reasons for the lower efficiency in UHPLC are most likely that the HPLC column was twice as long as the UHPLC one, the column loading was higher in the UHPLC experiments and that the extra-column volume in the UHPLC system was a larger fraction of the column volume. Temperature gradients causing a radial thermal heterogeneity and pressure gradients could also affect the efficiency.

Through the aid of the stochastic modelling and by $\ln(k)$ vs. $1/T$ and $\ln(k)$ vs. P plots we will try to investigate the individual contributions of temperature and pressure to retention and peak shape.

4.1 Temperature and pressure effects on retention

4.1.1 Pressure dependence

The slope of $\ln(k)$ vs. P_{avg} plots is equal to $\Delta V_m = V_{stat.} - V_{mob}$,i.e. the change in solute molar volume associated with the transition between the stationary and mobile phase [29]. Generally the solute molar volume is larger in the mobile phase, i.e. $\Delta V_m < 0$. According to Le Chatelier principle, when the pressure is increased the equilibrium between solute

281 molecules in the mobile and stationary phase will be pushed toward the stationary phase ,
282 resulting in increasing retention time [29,30].

283 The logarithm of the retention factor for different pressures was fitted with linear regression
284 and the result is presented in Fig. 2. The relationship between ln(k) and P_{avg} is linear with a R^2
285 value larger than 0.980. Calculated ΔV_m values were -11.9 ± 1.0 cm^3/mol for BTEAC, -15.5 ±
286 0.3 cm^3/mol for SNS, -3.4 ± 0.3 cm^3/mol for C7 and -18.4 ± 0.5 cm^3/mol for OM given with a
287 95% confidence interval. These observations are in good agreement with those reported by
288 Fallas et al. [10,11] for a similar system. The negative ΔV_m is attributed to the partial loss of
289 the solvation layer of the solutes when they move from the mobile to the hydrophobic
290 stationary phase. The difference in ΔV_m between uncharged and ionized solutes is believed
291 to be due to the hydration of the ions which are partially lost when entering the stationary
292 phase. However, this clearly shows that pressure is a factor that needs to be considered
293 because it could affect the selectivity as well as retention.

294 **4.1.2 Temperature dependence**

295 To better understand the effect of viscous he ating, the temperature gradients in the column
296 were quantified. The 2-dimensional temperature profile corresponding to UHPLC conditions
297 of 25% acetonitrile and flow rate 1.2 mL/min (same as Fig. 1) has been calculated and shown
298 in Fig. 3. The dotted line at 1.05 mm represents the inner column wall. Because the column
299 temperature profile was assumed to be radially symmetrical, only half of the temperature
300 contour plot is shown. As can be seen from Fig. 3, the temperature along the column, i.e.
301 longitudinally, increased ≃16°C from the inlet to the outlet and the temperature inside the
302 column from centrum to wall, i.e. radially, decreased ≃2°C at most. The values calculated for
303 this specific system are close to those reported in the literature [6,9] for similar pressure
304 drops over the column.

The effect of the temperature gradient on retention was estimated by calculating the local propagation speeds along the column by first calculating the geometric radial average temperature using the temperature profile in Fig. 3. Then the temperature dependence of the retention factor was determined by fitting the logarithm of retention factors to the reciprocal temperature, Fig. 4. Linearity of ln (k) vs. $1/T$ was observed in all cases with R^2-values above 0.990, except for BTEAC for which a slight nonlinearity was observed with R^2-value 0.960. The retention factor of all solutes decreases with temperature, which is the common behavior in RP-LC for moderate temperature variations. Combining this information the retention time was estimated by integrating the solute local propagation speed along the UHPLC column. The uncharged solute, C7, is least affected by the temperature gradient with a decrease in k of roughly 5%. The positively charged solute, BTEAC, is somewhat more sensitive and k decreases about 10% while the negatively charged solute, SNS, is most affected by temperature and k decreases almost 14%. The retention factor of OM decreases approximately 9%, which places it in the same region as the other two charged solutes.

4.1.3 The relative importance of temperature and pressure gradients

In an attempt to compare the relative importance of pressure and temperature on retention in UHPLC, the results from Sec. 4.1.1 and 4.1.2 have been combined in Fig. 5, where the retention factors of the four investigated molecules have been normalized against the respective retention factor at 0.13 mL/min (where pressure and temperature gradients are negligible). In Fig. 5, white bars show the estimated contribution for temperature, while gray bars show the pressure contribution, which has been estimated by assuming a linear pressure gradient over the column. Finally, black bars represent the observed, experimental retention factors found in UHPLC.

The pressure and temperature have opposite effects on retention and will therefore, to a certain degree, cancel each other. Under typical UHPLC conditions, the pressure effect is always larger than the temperature effect, except for C7. For C7, which is uncharged, the pressure effect is very small. Both the pressure and temperature effects are solute dependent. In particular, our data show that charged solutes and those with larger molecular weight are most affected by pressure. These results also suggest that in the method transfer from HPLC to UHPLC, especially if charged solutes are considered, the effect of the pressure gradient along the column more than that of temperature gradient should be taken into account, as it is the dominating one.

4.2 Stochastic Modelling

The adsorption isotherms for the modeling compounds has previously been investigated and it was found that C7 and OM exhibited homogeneous adsorption while SNS and BTEAC had heterogeneous adsorption [22]. Since the peak shape was also very symmetrical for C7, OM and SNS, they were described by 1-site stochastic models. One must stress that heterogeneous adsorption not necessarily results in measurable heterogeneous kinetics.

For very symmetrical peak shapes as those observed under our conditions, the number of adsorption/desorption events (n) and adsorption sojourn time (τ_s) are strictly correlated, so that nonlinear fitting cannot differentiate between them. Therefore, any trends with temperature or pressure seen for this kind of peaks may be an artifact of nonlinear fitting. As a consequence, only the range of these parameters is given here. The conclusion is that for solutes with very symmetrical peaks, the stochastic approach is unable to single out pressure and temperature effects.

For BTEAC, the elution peaks are asymmetrical so the nonlinear fitting could differentiate between contributions of n and τ_s.

353 **4.2.1 Temperature dependence**

354 For OM, C7 and SNS (1-site model) n is similar for all three solutes (10 000 to 20 000) in HPLC
355 and UHPLC with the values for UHPLC being slightly lower. τ_s is between 10 and 20 ms and
356 the values are slightly higher for UHPLC than for HPLC. These observations reflect the fact
357 that the measured column efficiency is higher in HPLC.

358 BTEAC adsorption is described by a 2-site adsorption isotherm [22] and the elution peaks are
359 tailing so the 2-site stochastic model has been employed to fit the chromatograms. Site-1 is
360 where the majority of all adsorption/desorption events take place and the sojourn time for
361 these sites are in the millisecond scale, Fig. 6. On the other hand, at site-2 only a few
362 adsorption/desorption events take place. However, the sojourn time found on these sites is
363 roughly one thousand times longer than on site-1. We observe that the average number of
364 adsorption/desorption events increases with increasing temperature and that the sojourn
365 time decreases with increases temperature for both sites and systems. From a fundamental
366 perspective, increasing the temperature will result in an increased diffusion coefficient both
367 due to the temperature itself but also due to a reduction in viscosity, as described by the
368 Stokes–Einstein equation. The faster kinetics will result in increased n and decreased τ_s as
369 observed. The scatter of the data points in Fig. 6, especially for n_1 and n_2, is most likely due
370 to a combination of numerical errors in the optimization and experimental errors.

371 The skew can be seen as a measure of the peak symmetry where a large positive skew
372 means that the peak is tailing and a negative skew means that the peak is fronting. In this
373 case the skew decreases with temperature for both HPLC and UHPLC, Fig. 6f, which indicates
374 that the peak shape becomes more symmetrical when the temperature is increased.
375 Relating the observation of decreasing skew to Eq. 3b, it is due to the increase in n_2 and the
376 decrease in $\tau_{s,2}$ for the slow site with increasing temperature. This also clearly shows that the
377 tailing observed for BTEAC (see Fig. 1) is due to heterogeneous kinetics.

4.2.2 Pressure dependence

For C7, OM and SNS, that is the compounds described by 1-site stochastic model, n has been found to be nearly constant while τ_s increase slightly with increasing pressure. In particular, n was between 8000 and 14000 and τ_s between 10 and 22 ms. It has previously been reported that increasing pressure could result in decreasing efficiency [20]. One probable explanation to this could be that the viscosity increases with the pressure [31] and as a result through the Stokes–Einstein equation this will result in an increased diffusion coefficient. From the stochastic model perspective this will result in reduction in n because slower diffusion results in fewer adsorption/desorption events take place. The sojourn time (τ_s) will increase because it takes longer time for the solute to diffuse out from the stationary phase. In this study for C7, OM and SNS we observed an increasing sojourn time but more or less no effect on n.

The results for BTEAC are presented in Fig. 7 and show that on the "fast" adsorption site there is an increase of n_1 and a decrease in $\tau_{s,1}$. While the "slow", second site, presents a nearly 50% increase in $\tau_{s,2}$ with a 500 bar pressure increase. As a consequence, the peak skew is increased, Fig. 7f and efficiency decrease when the pressure is increased, Fig. 7e. This increase in peak skew is due to the fact that the solute molecules spend on average a longer time adsorbed on the slow, second site when the pressure increases which makes the tailing more pronounced. To understand heterogeneous kinetics pressure dependency better it should be necessary to include more experiments with focus on several different kinds of basic compounds, however this is outside the scope of the study. So the presented result should be viewed as a first observation.

From Fig. 6 and Fig. 7, one may conclude that high temperature and low pressure improve peak shape for BTEAC. We believe that, even though more information must be gathered to draw any general conclusions, this is an interesting finding.

4.3 Practical implications

To compare the performance of HPLC and UHPLC, retention time, column efficiency and resolution for a degraded omeprazole sample containing the degradation product H168/66 in small amounts were investigated. The same mobile phase, temperature and stationary phase chemistry were used. The column dimensions and particle diameters differed; the HPLC column was 100 × 4.6 mm, 3.5 µm and the UHPLC column was 50 × 2.1 mm, 1.7 µm. The flow rate and injection volume for HPLC was 2.0 mL/min and 10 µL and for UHPLC they were scaled according to ref. [32] which yielded 0.86 mL/min and 1 µL. The scaling was done to keep the reduced linear velocity of the mobile phase constant. At these flow rates the pressure drop over the HPLC column was 165 bar and 570 bar over the UHPLC column.

The chromatograms are presented in Fig. 8, where the retention time for omeprazole is 3.6 longer in HPLC. The retention times, efficiencies (moment method) and resolution factors (half-height) are presented in Table 2. The efficiency of omeprazole was 29% higher in HPLC and efficiency for H168/66 was 13% higher, which resulted in a resolution factor that was about 9% higher in HPLC. However, the loss in efficiency and resolution when switching to UHPLC are very minor compared to the reduction in run time and resulting decrease in solvent consumption which makes UHPLC the primary choice in this case. The individual effects of pressure and temperature gradients in UHPLC are not directly observable since their effects are convoluted when comparing the different modes in this way.

5. Conclusions

The aim of this study has been to investigate how pressure and temperature affect retention and peak shape of the solutes in HPLC and UHPLC. To this end, the chromatographic behavior of four model compounds with different physicochemical properties has been modeled from both a thermodynamic and a kinetic (microscopic-stochastic) viewpoint. The

thermodynamic models showed that the difference in solute molar volume for adsorbed and in bulk solution, which determines the pressure dependence of the retention factor, was largest for the polar solute omeprazole which also had the largest molecular weight. When combining the calculated temperature gradient and the linear pressure gradient the individual contributions on retention could be determined. The effect of the pressure gradient was found to be the dominating one and should therefore be taken into account when switching from HPLC to UHPLC.

From the stochastic modelling of the tailing, basic solute it was evident that an increase in temperature yielded an increase in average number of adsorption/desorption events while the average time spent by a molecule in the stationary phase was slightly decreasing. For increased pressure the effect was the opposite. Therefore a high temperature and a low pressure yielded low tailing. Even though from different perspectives, the conclusions of these models converge in showing that the effect of pressure gradient along the column is as important as that of viscous heating. With charged and polar compounds, we found that the impact of the pressure gradient is even more important than that of viscous heating in UHPLC for the investigated experimental conditions.

Acknowledgement

We are grateful to Waters that provided an ACQUITY UPLC H-Class system with support and technical advice during the project. We are also grateful to Anders Karlsson at AstraZeneca R&D Mölndal for initiating this project and for most valuable discussions. This work was supported by the Swedish Research Council (VR) in the project "Fundamental studies on molecular interactions aimed at preparative separations and biospecific measurements" (grant number 621-2012-3978) and by the Swedish Knowledge Foundation for the KK HÖG 2014 project "SOMI: Studies of Molecular Interactions for Quality Assurance, Bio-Specific

Measurement & Reliable Supercritical Purification" (grants number 20140179). AC thanks the Italian University and Scientific Research Ministry (PRIN 2012ATMNJ_003).

References

[1] S. Fekete, J. Schappler, J.-L. Veuthey, D. Guillarme, Current and future trends in UHPLC, TrAC. 63 (2014) 2–13.
[2] S. Fekete, E. Oláh, J. Fekete, Fast liquid chromatography: The domination of core–shell and very fine particles, J. Chromatogr. A. 1228 (2012) 57–71.
[3] M. Szalka, J. Kostka, E. Rokaszewski, K. Kaczmarski, Analysis of related substances in bisoprolol fumarate on sub-2-µm adsorbents, Acta Chromatogr. 24 (2012) 163–183.
[4] S. Fekete, J.-L. Veuthey, D.V. McCalley, D. Guillarme, The effect of pressure and mobile phase velocity on the retention properties of small analytes and large biomolecules in ultra-high pressure liquid chromatography, J. Chromatogr. A. 1270 (2012) 127–138.
[5] H. Poppe, J.C. Kraak, Influence of thermal conditions on the efficiency of high-performance liquid chromatographic columns, J. Chromatogr. 282 (1983) 399–412.
[6] F. Gritti, G. Guiochon, Complete Temperature Profiles in Ultra-High-Pressure Liquid Chromatography Columns, Anal. Chem. 80 (2008) 5009–5020.
[7] F. Gritti, M. Martin, G. Guiochon, Influence of Viscous Friction Heating on the Efficiency of Columns Operated under Very High Pressures, Anal. Chem. 81 (2009) 3365–3384.
[8] K. Kaczmarski, J. Kostka, W. Zapała, G. Guiochon, Modeling of thermal processes in high pressure liquid chromatography: I. Low pressure onset of thermal heterogeneity, J. Chromatogr. A. 1216 (2009) 6560–6574.
[9] K. Kaczmarski, F. Gritti, J. Kostka, G. Guiochon, Modeling of thermal processes in high pressure liquid chromatography: II. Thermal heterogeneity at very high pressures, J. Chromatogr. A. 1216 (2009) 6575–6586.
[10] M.M. Fallas, U.D. Neue, M.R. Hadley, D.V. McCalley, Investigation of the effect of pressure on retention of small molecules using reversed-phase ultra-high-pressure liquid chromatography, J. Chromatogr. A. 1209 (2008) 195–205.
[11] M.M. Fallas, U.D. Neue, M.R. Hadley, D.V. McCalley, Further investigations of the effect of pressure on retention in ultra-high-pressure liquid chromatography, J. Chromatogr. A. 1217 (2010) 276–284.
[12] J.C. Giddings, H. Eyring, A molecular dynamic theory of chromatography, J. Phys. Chem. 59 (1955) 416–421.
[13] F. Dondi, M. Remelli, The characteristic function method in the stochastic theory of chromatography, J. Phys. Chem. 90 (1986) 1885–1891.
[14] A. Cavazzini, M. Remelli, F. Dondi, Stochastic Theory of Two-Site Adsorption Chromatography by the Characteristic Function Method, J. Microcol. Sep. 9 (1997) 295–302.
[15] A. Cavazzini, M. Remelli, F. Dondi, A. Felinger, Stochastic Theory of Multiple-Site Linear Adsorption Chromatography, Anal. Chem. 71 (1999) 3453–3462.
[16] A. Felinger, Molecular movement in an HPLC column: A stochastic analysis, LCGC N. A. 22 (2004) 642–647.
[17] M. Enmark, J. Samuelsson, T. Undin, T. Fornstedt, Characterization of an unusual adsorption behavior of racemic methyl-mandelate on a tris-(3,5-dimethylphenyl) carbamoyl cellulose chiral stationary phase, J. Chromatogr. A. 1218 (2011) 6688–6696.

[18] F. Dondi, A. Cavazzini, M. Remelli, A. Felinger, M. Martin, Stochastic theory of size exclusion chromatography by the characteristic function approach, J. Chromatogr. A. 943 (2002) 185–207.
[19] K. Horváth, M. Olajos, A. Felinger, P. Hajós, Retention controlling and peak shape simulation in anion chromatography using multiple equilibrium model and stochastic theory, J. Chromatogr. A. 1189 (2008) 42–51.
[20] K. Okusa, Y. Iwasaki, I. Kuroda, S. Miwa, M. Ohira, T. Nagai, et al., Effect of pressure on the selectivity of polymeric C18 and C30 stationary phases in reversed-phase liquid chromatography. Increased separation of isomeric fatty acid methyl esters, triacylglycerols, and tocopherols at high pressure, J. Chromatogr. A. 1339 (2014) 86–95.
[21] F. Gritti, G. Guiochon, Adsorption Mechanisms and Effect of Temperature in Reversed-Phase Liquid Chromatography. Meaning of the Classical Van't Hoff Plot in Chromatography, Anal. Chem. 78 (2006) 4642–4653.
[22] D. Åsberg, M. Leśko, J. Samuelsson, K. Kaczmarski, T. Fornstedt, Method transfer from high-pressure liquid chromatography to ultra-high-pressure liquid chromatography. I. A thermodynamic perspective, J. Chromatogr. A. 1362 (2014) 206–217.
[23] A. Felinger, Molecular dynamic theories in chromatography, J. Chromatogr. A. 1184 (2008) 20–41.
[24] J.C. Giddings, Dynamics of chromatography: principles and theory, Marcel Dekker, New York, 1965.
[25] E. Morgan, K.W. Burton, G. Nickless, Optimization using the super-modified simplex method, Chemometr. Intell. Lab. Syst. 8 (1990) 97–107.
[26] F. Gritti, G. Guiochon, Mass transfer mechanism in chiral reversed phase liquid chromatography, J. Chromatogr. A. 1332 (2014) 35–45.
[27] J. Billen, K. Broeckhoven, A. Liekens, K. Choikhet, G. Rozing, G. Desmet, Influence of pressure and temperature on the physico-chemical properties of mobile phase mixtures commonly used in high-performance liquid chromatography, J. Chromatogr. A. 1210 (2008) 30–44.
[28] M. Martin, G. Guiochon, Effects of high pressure in liquid chromatography, J. Chromatogr. A. 1090 (2005) 16–38.
[29] V.L. McGuffin, S.-H. Chen, Molar enthalpy and molar volume of methylene and benzene homologues in reversed-phase liquid chromatography, J. Chromatogr. A. 762 (1997) 35–46.
[30] P. Atkins, J. De Paula, Physical Chemistry, 9th ed., Oxford University Press, Oxford, 2010.
[31] M. Martin, G. Guiochon, Effects of high pressure in liquid chromatography, J. Chromatogr. A. 1090 (2005) 16–38.
[32] D. Guillarme, D.T.-T. Nguyen, S. Rudaz, J.-L. Veuthey, Method transfer for fast liquid chromatography in pharmaceutical analysis: Application to short columns packed with small particle. Part I: Isocratic separation, Eur. J. Pharm. Biopharm. 66 (2007) 475–482.

Figure captions

Fig. 1: Overlaid chromatograms for HPLC (black) and UHPLC (gray). All extra-column volumes have been corrected for and the retention volumes have been normalized with the HPLC and UHPLC column volumes, respectively. The column temperature was set to 40°C and the

pressure drop over the column in HPLC was 100 bar and in UHPLC 800 bar, respectively. This corresponded to a flow rate of 1.0 mL/min for HPLC and 1.2 mL/min for UHPLC.

Fig. 2: Experimental retention factors for BTEAC (circles), C7 (squares), SNS (diamonds), and OM (triangles) for different pressures. Mobile phase compositions were 7, 15 and 25% acetonitrile for BTEAC, SNS and C7/OM, respectively and flow rate was 0.13 mL/min.

Fig. 3: Calculated temperature profile in UHPLC for the mobile phase 25/75, v/v acetonitrile/phosphate buffer at flow rate 1.2 mL/min. The dotted line represents the inner column wall. At 50 mm the center of the column is warmest (55°C) and the column wall is at ca 52°C; radius 0 is the center of the column. The pressure over the column is 782 bar.

Fig. 4: Experimental retention factors for BTEAC (circles), C7 (squares), SNS (diamonds), and OM (triangles) for different temperatures. Mobile phase compositions were 7, 15 and 25% acetonitrile for BTEAC, SNS and C7/OM, respectively and flow rate was 0.13 mL/min.

Fig. 5: The retention factor is compared for four different cases in UHPLC. The baseline is taken as the retention factor at low flow rate 0.13 mL/min where pressure and temperature gradients are negligible; the bars denoted "only *T*" represent the effect caused only by the temperature gradient; "only *P*" denotes the case with only the pressure effect present and "observed" represents actual experimental result where both pressure and temperature effects are present.

Fig. 6: Stochastic modelling of BTEAC which is described by a 2-site model at different temperatures. *N* is the column efficiency determined with Eq. 4 and *S* is the skew determined with Eq. 3b.

Fig. 7: Stochastic modelling of BTEAC which is described by a 2-site model at different pressures. *N* is the column efficiency determined with Eq. 4 and *S* is the skew determined with Eq. 3b.

Fig. 8: Chromatogram from HPLC and UHPLC for omeprazole (large peak) and the degradation product H168/66 (small peak) for identical mobile phase, stationary phase and column temperature. Flow rates are 2 mL/min in HPLC and 0.86 mL/min in UHPLC.

Table 1:
Physicochemical properties from the manufacturer of the columns

Property	**XBridge BEH-C_{18}**	**AQUITY BEH-C_{18}**
Average particle size [µm]	3.5	1.7
Pore volume [cm^3/g]	0.71	0.70
Surface area [m^2/g]	184	179
Average pore diameter [Å]	138	141
Total carbon content [%]	17.88	17.40
Surface concentration [$\mu mol/m^2$]	3.36	3.07

Table 4: Parameters for the separation of omeprazole and the degradation product H168/66 using HPLC and UHPLC columns, respectively. t_r is the retention time, N the efficiency and R_s the resolution factor.

Solute	**Parameter**	**HPLC**	**UHPLC**
OM	t_r [min]	2.61	0.72
H168/66	t_r [min]	1.74	0.45
OM	N	5970	4230
H168/66	N	6240	5460
-	R_s	9.87	8.99

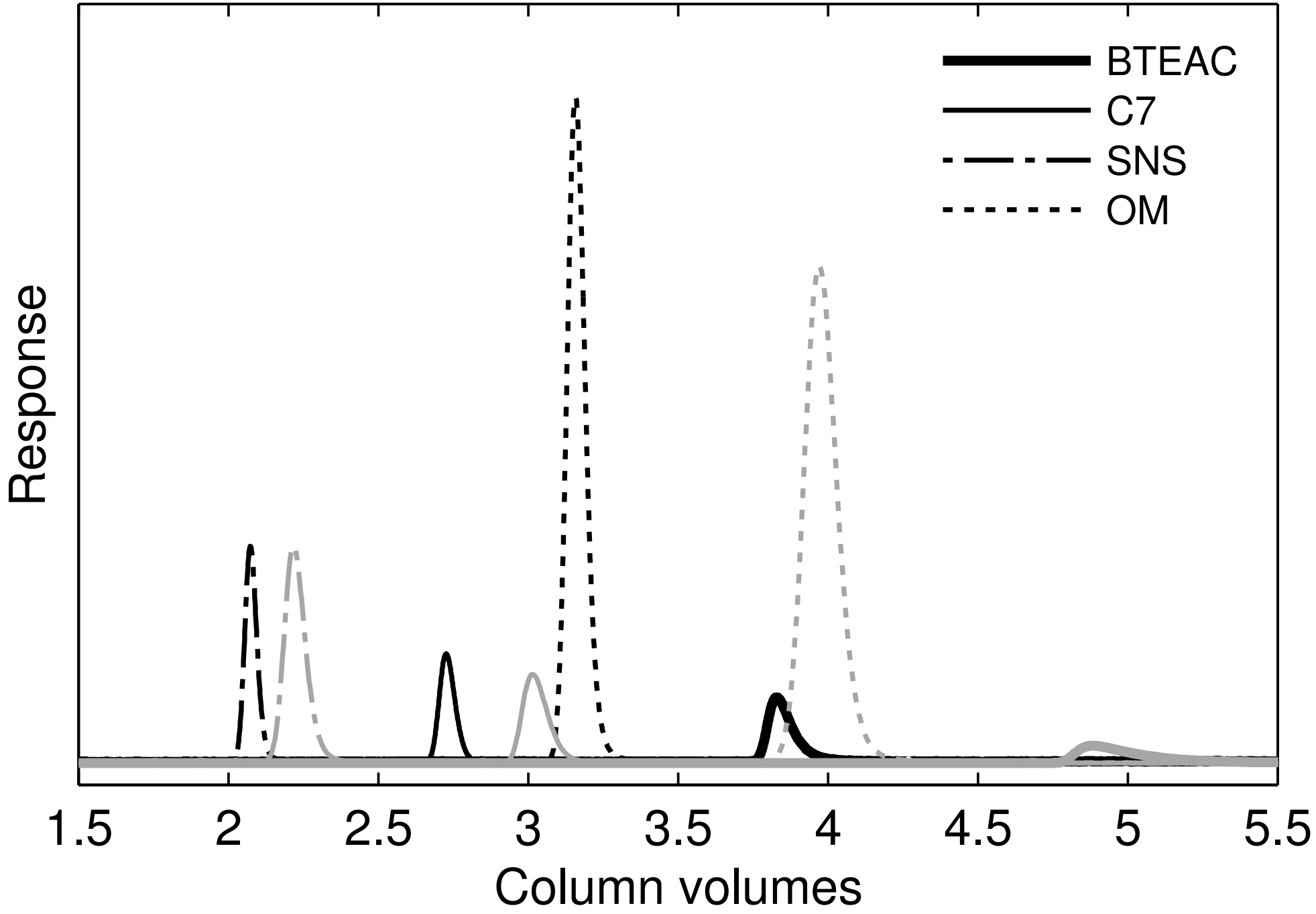
BTEAC
C7
SNS
OM
Response
1.5
2
2.5
3
3.5
4
4.5
5
5.5
Column volumes

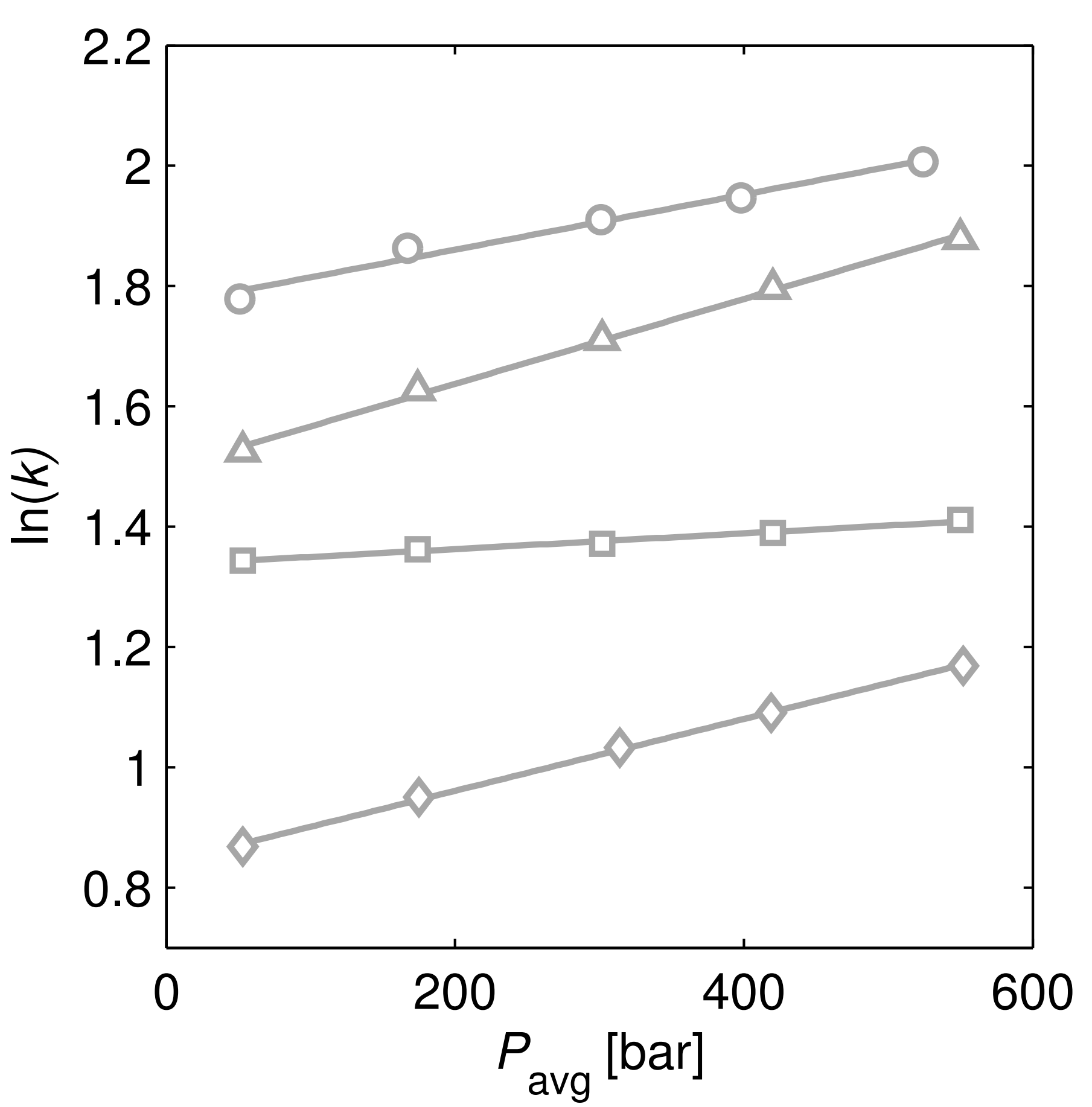
2.2
2
1.8
1.6
1.4
1.2
1
0.8
ln(k)
0
200
400
600
P avg [bar]

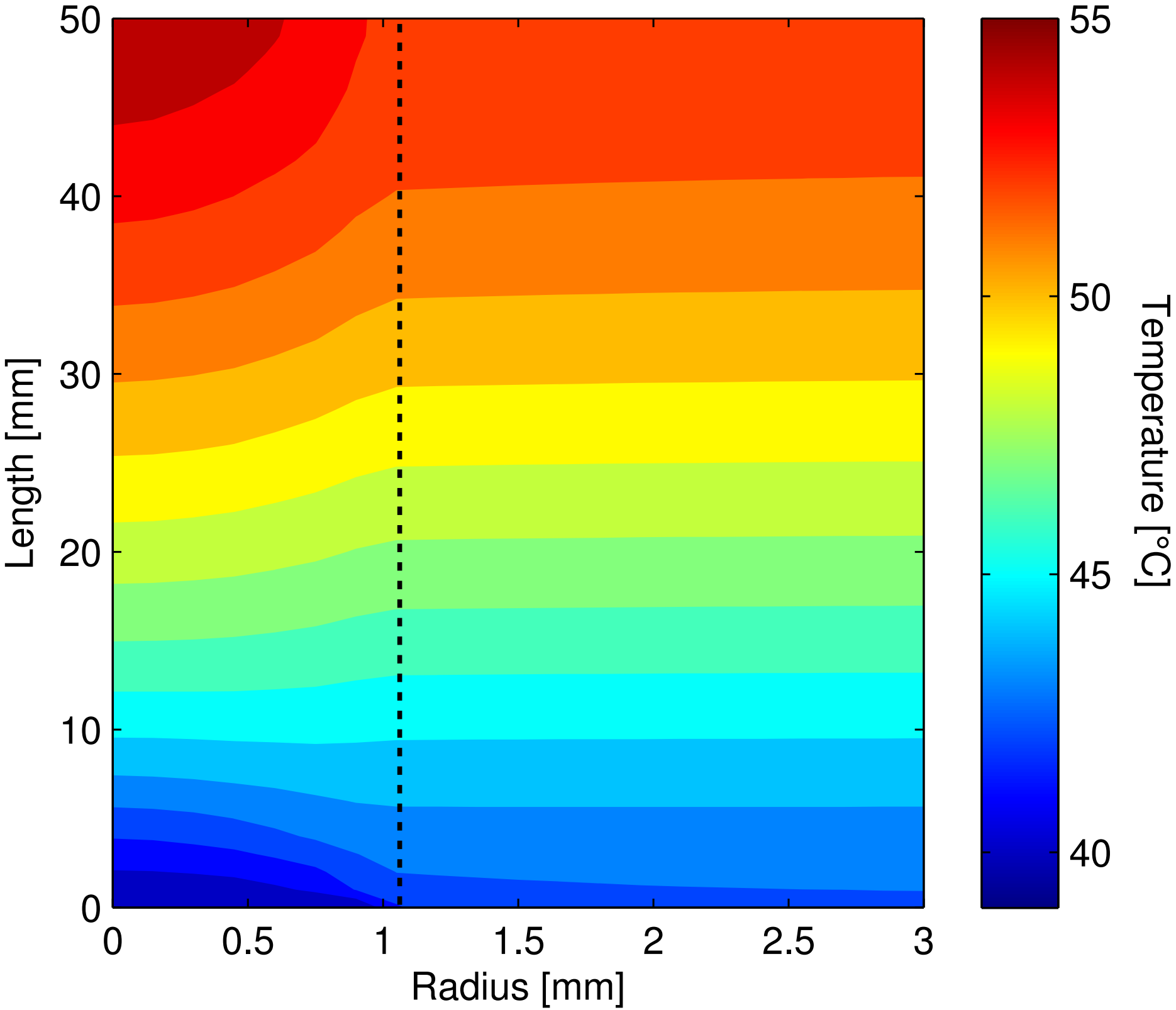
50
40
30
20
10
0
Length [mm]
0
0.5
1
1.5
2
2.5
3
Radius [mm]
55
50
45
40
Temperature [°C]

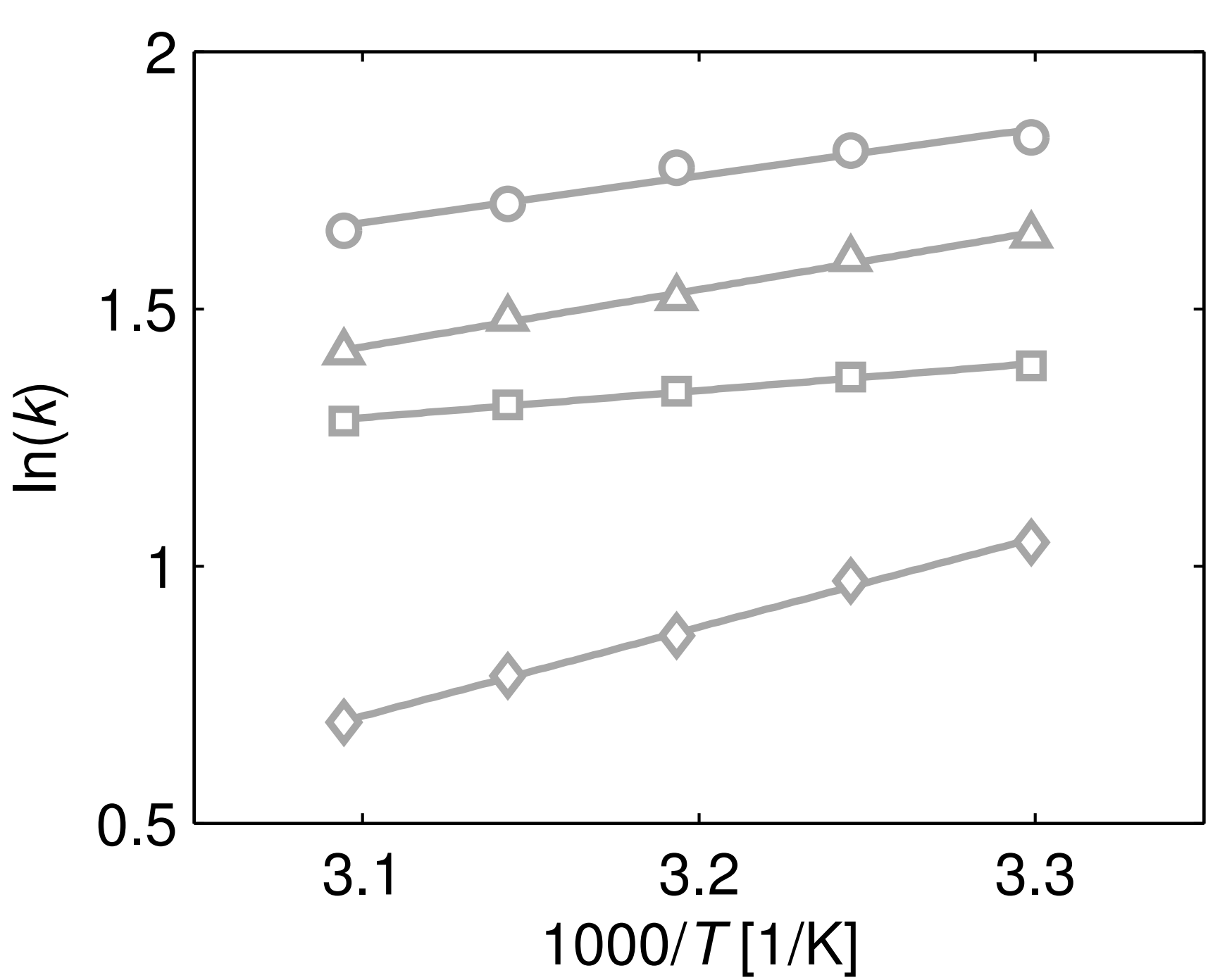
2
1.5
1
0.5
ln(k)
3.1
3.2
3.3
1000/T [1/K]

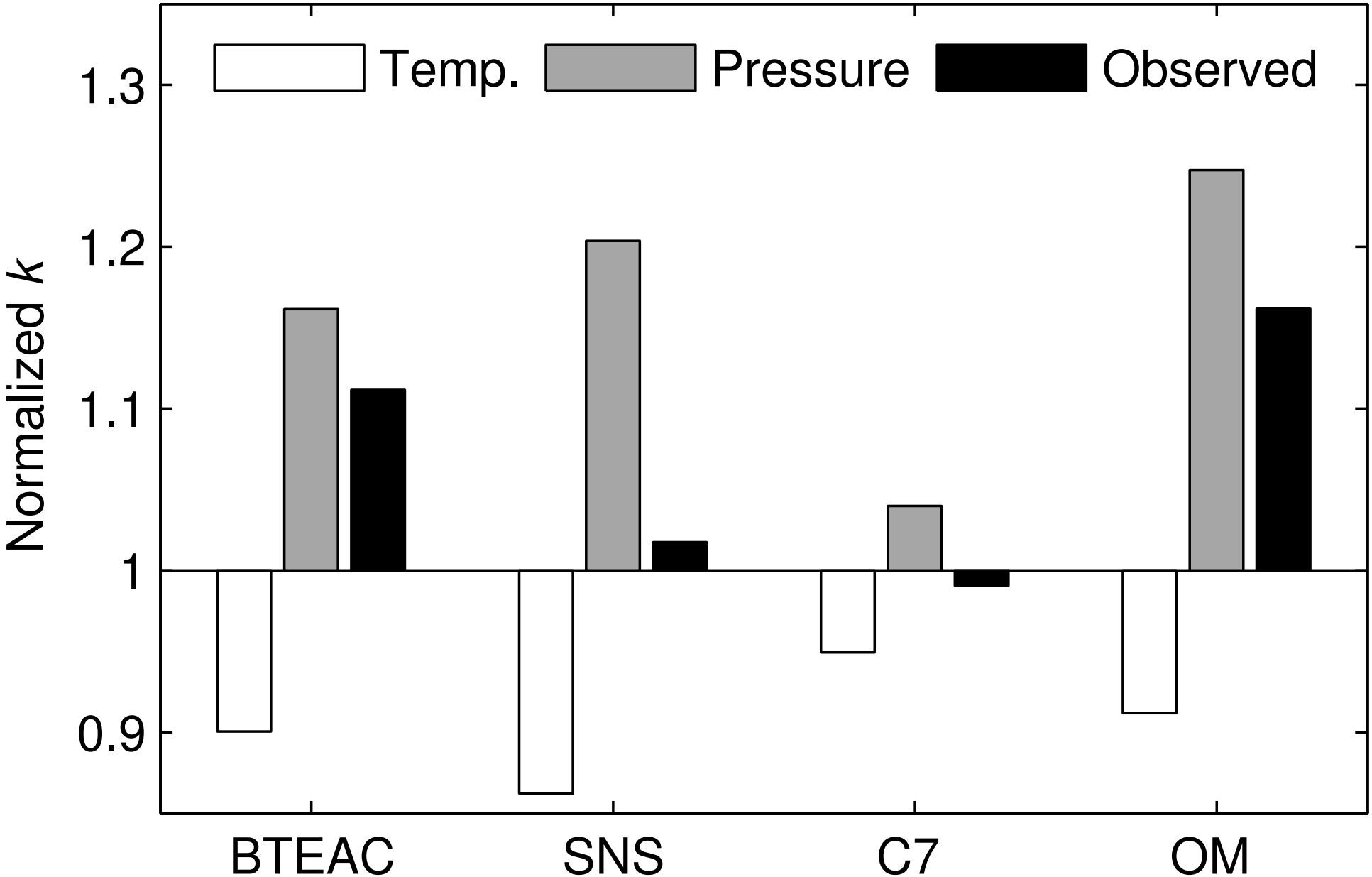
Temp.
Pressure
Observed
Normalized k
1.3
1.2
1.1
1
0.9
BTEAC
SNS
C7
OM

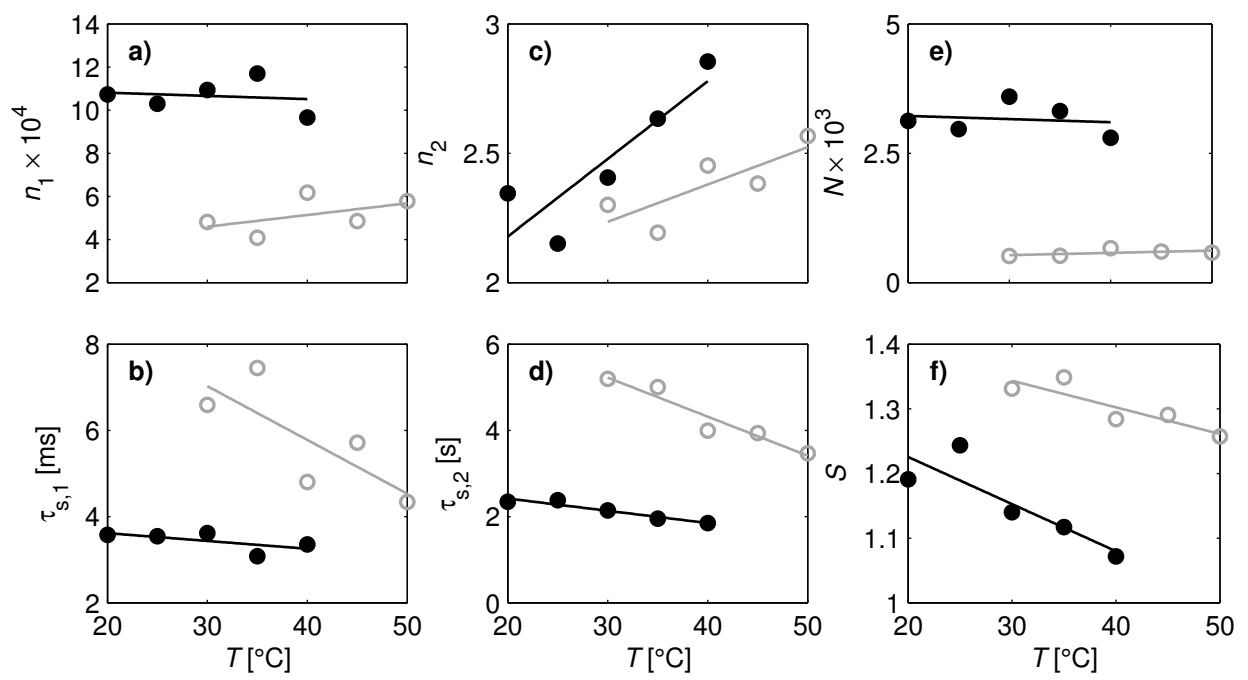
a)
b)
c)
d)
e)
f)
$n_1 \times 10^4$
$\tau_{s,1}$ [ms]
n_2
$\tau_{s,2}$ [s]
$N \times 10^3$
S
T [°C]
T [°C]
T [°C]

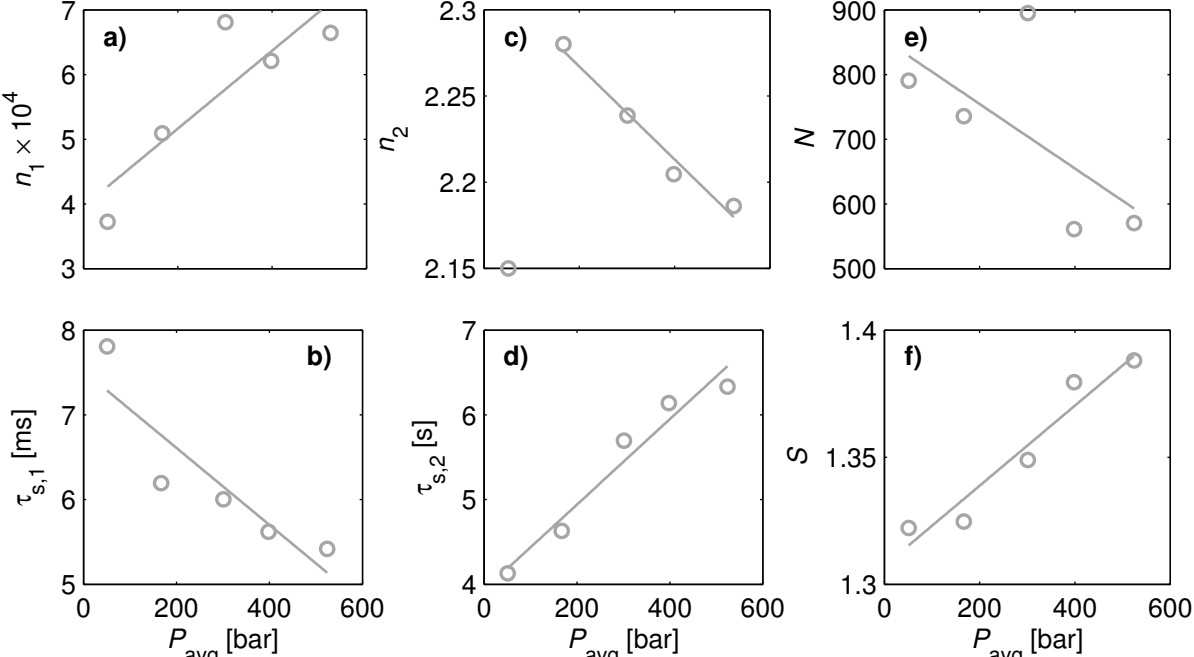
a)
$n_1 \times 10^4$
7
6
5
4
3
c)
n_2
2.3
2.25
2.2
2.15
e)
N
900
800
700
600
500
b)
$\tau_{s,1}$ [ms]
8
7
6
5
d)
$\tau_{s,2}$ [s]
7
6
5
4
f)
S
1.4
1.35
1.3
0
200
400
600
P_{avg} [bar]

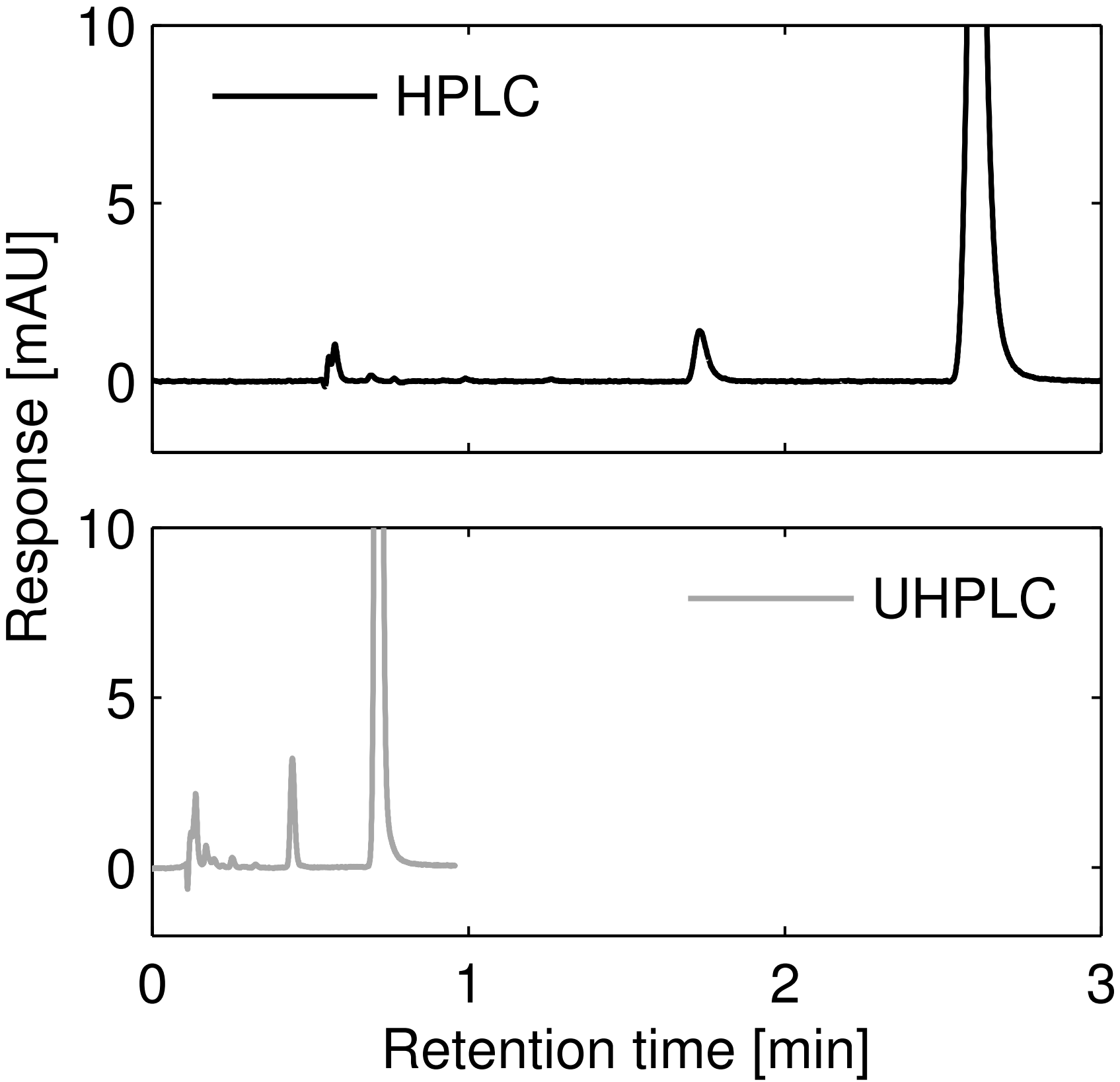
HPLC
UHPLC
Response [mAU]
Retention time [min]
10
5
0
10
5
0
0
1
2
3